Journal of Materials Chemistry A

Accepted Manuscript

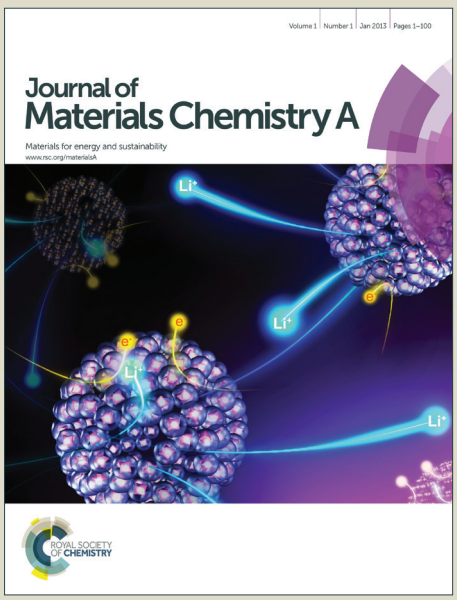

ROYAL SOCIETY OF CHEMISTRY

www.rsc.org/materialsA

Table of Contents Entry

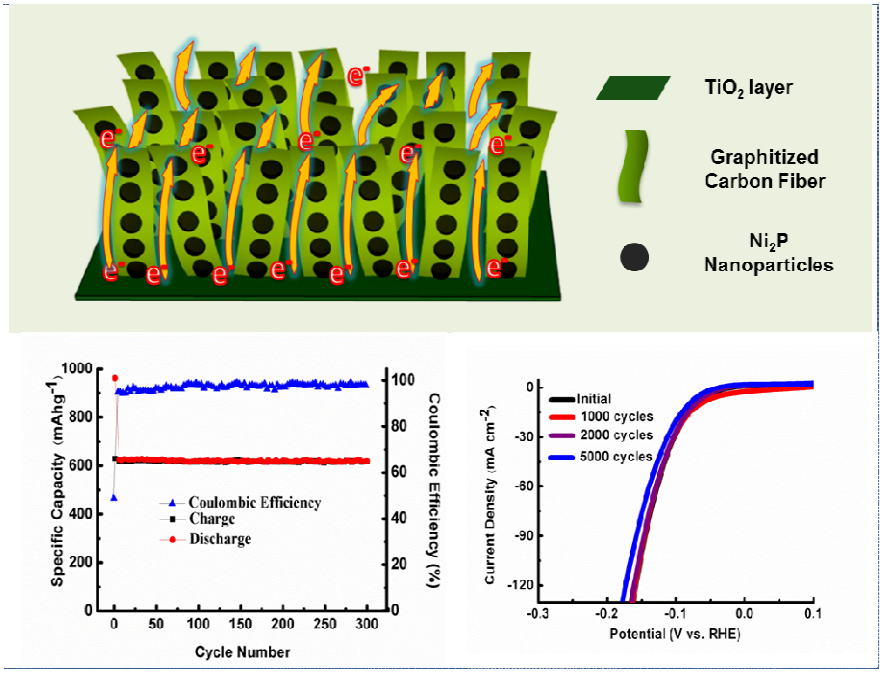

Recently, Ni_2P-based nanomaterials have attracted considerable attention due to their unique properties and applications specially related to anode materials for Li ion batteries (LIBs) and electrocatalysts for hydrogen evolution reaction. In this work we report, for the first time, the controlled synthesis of one-dimensional (1D) peapods array of Ni_2P@graphitized carbon fiber composites grown directly on Ti foil substrate through a simple hydrothermal reaction followed by a thermal annealing process. The electrode architecture takes advantages of the 1D peapods array composed of the outer layer of graphitized carbon fiber and the encapsulated Ni_2P nanoparticles, and Ti conductive substrate, leading to outstanding electrochemical performance. It is believed that the designed synthesis of the novel architecture would offer new insights into the preparation of 1D peapod array materials, and provides promising opportunities in their applications in electrochemical devices.

Novel Peapods Array of Ni_2P@Graphitized Carbon Fiber Composites Growing on Ti Substrate: A Superior Material for Li-Ion Batteries and Hydrogen Evolution Reaction

*Yuanjuan Bai, Huijuan Zhang, Ling Fang, Li Liu, Huajun Qiu, Yu Wang**

The State Key Laboratory of Mechanical Transmissions and the School of Chemistry and Chemical Engineering, Chongqing University, 174 Shazheng Street, Shapingba District, Chongqing City, P.R. China, 400044

E-mail: wangy@cqu.edu.cn; prospectwy@gmail.com

Supporting information for this article is available.

Keywords: Peapods Array, Ni_2P, LIBs, Anode, Hydrogen Evolution Reaction

A novel one-dimensional (1D) peapods array of Ni_2P@graphitized carbon fiber composites consisting of graphitized carbon fiber and the encapsulated Ni_2P nanoparticles has been designed and synthesized on Ti foil substrate. This smart and elaborate architecture design offers several remarkable advantages, including large interfacial area, short charge transporting path, strong physical adhesion with the current collector and large electrolyte's diffusion pathway between the peapods array. When used for LIBs, excellent electrochemical performances such as high capacity of 634 mAh g^{-1} at a current density of 200 mA g^{-1}, long-term cycling stability and outstanding rate capability, are obtained. In 0.5 M H_2SO_4, as electrocatalyst for HER, the peapods array of Ni_2P@graphitized carbon fiber composites affords a current density of 10 mA cm^{-2} at a small over-potential of 45 mV and a small Tafel slope of~46 mV/decade. Importantly, the sample exhibits exceptional stability in acidic environment. Moreover, it is believed that the idea to prepare the 1D peapods array on conductive substrate is general and could be extended to other materials.

Introduction

To our knowledge, design and synthesis of nanomaterial with superior physicochemical properties has great potentials for many applications such as electrochemical energy storage, catalysis and so on.[1-4] However, it should be noteworthy that the structures and morphologies of materials have a great impact on their performance. So far, many attempts, including minimizing the particle size, coating the active materials with electrically conductive layers, and adopting metal substrates as current collectors, have been made to tailor the architectures and shapes. Derived from the strategy, some functional nanomaterials with special morphologies, such as sandwich-like nanocomposite architecture,[5] three-dimensional (3D) hierarchical structure,[6] yolk-shell hetero-structures[7] and peapod-like structure[8] have been developed and widely applied in various areas. Especially, the novel one-dimensional (1D) peapod-like material gains tremendous attention due to their intriguing architectural features.[8-10] The advantages of this peapod-like structure includes a larger surface area to enhance the interfacial kinetics, a sufficient space to accommodate the stress relaxation and a fluent pathway for charge transport. These attractive features are of great significance to improve the electrochemical performance.

Up to now, it has been shown that nanostructure arrays directly grown on conductive metal substrates could provide desirable LIB anodes and catalyst of hydrogen evolution reaction (HER) because of their significant advantages, for instance, short charge transporting path, high surface-to-volume ratio, vectorial electron-transport property, good contact between the active materials and current collector, which are essential to develop high-performance electrode materials. For example, You et al. synthesized 1D hierarchical Fe_3O_4/CuO hybrid wires on a copper substrate, which displayed high reversible specific capacity, good cycling stability (delivering a discharge capacity of 953 mAh g^{-1} during the 100^{th} cycle at 820 mA g^{-1}) and high rate capabilities (319 mAh g^{-1} at 8200 mA g^{-1}), superior to those of their individual building blocks Fe_3O_4 and CuO.[11] Xue et al. prepared porous

Co_3O_4 nanoneedle array on copper foils and achieved the ultra-fast charging/discharging and high capacity.[12]Jaramillo et al. prepared core-shell MoO_3-MoS_2 nanowires that efficiently drive the HER with stability over thousands of cycles.[13]Sun et al. developed a novel self-supported Cu_3P nanowire arrays on porous copper foam (Cu_3P NW/CF). As HER electrocatalyst in acidic solution, the Cu_3P NW/CF maintained its activity for at least 25 hours and showed an onset overpotential of 62 mV, a Tafel slope of 67 mV dec^{-1}, and nearly 100 % Faradaic efficiency (FE) as well.[14] These research findings indicate that the 1D nanostructure active materials could be effectively immobilized on conductive substrate during the preparation.

In recent years, transition metal phosphides (TMPs, where M = Fe, Co, Ni, Cu, etc.) have garnered considerable attention for their potential to facilitate both fundamental research and practical applications through their advantageous chemical and physical properties.[15-18] Ni_2P is a unique material with widespread technological applications, particularly used as catalysts for hydrodesulfurization (HDS), drodenitrogenation (HDN) and HER.[19-21]As HER catalyst, the Ni_2P nanostructures have an outstanding activity, producing H_2(g) with nearly quantitative faradaic yield, and also affording stability in aqueous acidic media.[21]Meanwhile, the Ni_2P nanostructures present excellent electrochemical properties as anode materials for Li-ion batteries (LIBs).[22] These excellent properties are related to their low polarization and resistivity, large active sites density and so on. Unfortunately, to this day, the rational design and controllable synthesis of nanostructured Ni_2P with superior lithium storage or electrocatalytic performance still remains a significant challenge.

Herein, by designing and controlling the morphology and structure of the nickel phosphide (Ni_2P), we have synthesized a novel 1D Ni_2P@graphitized carbon fiber composite peapods array on a Ti substrate based on our recent success to fabricate hierarchical Co_3O_4 nanoparticles@graphitized carbon fibers peapoded array on Ti foil and peapod-like Ni_2P/C nanocomposite.[10,23] As expected, the product is used directly as a binder-free electrode for LIBs and shows high capacity, long lifetime and excellent rate performance. The peapods array also shows enhanced electrocatalytic activity for electrochemical hydrogen evolution from water. The new achievement has widened the scope of 1D peapod array growing on metal conductive substrate and is meaningful to find more applications in chemistry and materials sciences.

Results and Discussion

Strategies for the synthesis of the $NH_4NiPO_4H_2O$ nanobelts and the peapods array of Ni_2P@graphitized carbon fiber composites are illustrated in Figure 1. First, the $NH_4NiPO_4H_2O$ nanobelts are synthesized on a piece of Ti foil through a hydrothermal process in a high-temperature oven. Ti foil is chosen as the substrate for the growth of arrays because of its high electronic conductivity. Here, Ti foil is usually covered with a thin layer of TiO_2. The reason is that the Ti foil is easy to be oxidized when it exposed to air. The isoelectric point with pH value for TiO_2 often falls into a range of 4.5–6.5.[24] In our experiment, the high-concentration ammonia is chosen to form a basic condition, leading to a large amount of hydroxyl groups on the Ti foil, which may be the centers of crystallization for $NH_4NiPO_4H_2O$.As a result, large-scale and ordered $NH_4NiPO_4H_2O$ nanobelts arrays are grown on Ti conductive substrates. Hydrate, as an important constituent for $NH_4NiPO_4H_2O$ molecules, offers the possibility of hydrogen bonding between glucose and $NH_4NiPO_4H_2O$ nanobelts. The hydrogen bonding interaction plays a vital role in coating the polymeric layer on $NH_4NiPO_4H_2O$ nanobelts through the hydrothermal reaction. In this research, the polymeric layer is prepared by hydrothermal treatment of precursor in glucose aqueous solution (1 M) in a sealed Teflon-lined stainless steel autoclave at 180 ℃ for 8 h. Finally, Ni_2P@graphitized carbon fiber composites peapods array can be obtained by heating the intermediate product at 700 ~ 750 ℃ in H_2 atmosphere. In this process, the coated carbon layer and reducing gas (H_2) play important role as reducing agents in the formation of the peapods structure and the reduction of $NH_4NiPO_4H_2O$ to Ni_2P, and the accompanying evolution of H_2O, P, CO or CO_2 will definitely result in a porous structure across the surface of the carbon fiber layer.

Figure 2 illustrates a series of the top-viewed and cross-sectional scanning electron microscopy (SEM) images

of $NH_4NiPO_4H_2O$ nanobelts array (a-b) and 1D Ni_2P@graphitized carbon fiber composites peapods array (c-d) uniformly grown on a Ti foil substrate. Importantly, only by using the powerful ultrasound technology could the $NH_4NiPO_4H_2O$ nanobelts and Ni_2P peapods arrays be scraped off the Ti foil, because there is a strong adhesion between the nanostructures' array and substrate. Meanwhile, the 1D array morphology is perfectly retained after thermal transformation. The morphological and structural details of the nanobelts are further characterized by SEM, transmission electron microscopy (TEM) and high-resolution TEM (HRTEM) as shown in Figure 3 and Figures S1 (Supporting Information). The precursor exhibits uniform belt-shaped morphology with lengths up to several micrometers and diameters approaching 50 nm (Figure 3a and Figure S1a-c, Supporting Information). From Figure 3b and Figure S1d (Supporting Information), it can be seen that the dispersed nanobelts possess single crystallinity with an inter-spacing of 0.88 nm, corresponding to the (010) crystal plane. Besides, as shown in Figure S2 (Supporting Information), the X-ray diffraction (XRD) patterns have successfully recorded the overall transition from $NH_4NiPO_4H_2O$ nanobelts array to Ni_2P peapods array on Ti foil, further certifying the rationality and reasonability of the designed synthesis of the unique 1D Ni_2P peapods array on conductive Ti substrate via the evolution of $NH_4NiPO_4H_2O$ nanobelts array. A HRTEM image in Figure S3a (Supporting Information) shows that the polymeric layer from glucose polymerization has successfully been coated on the $NH_4NiPO_4H_2O$ nanobelt surface.

To investigate the morphological and geometrical structural details of the 1D Ni_2P@graphitized carbon fiber peapods, we scraped off the products from Ti foil by using the powerful ultrasound technology. Figure 4a-b shows the typical SEM images of Ni_2P peapods with different magnifications. It can be clearly observed the product is peapod-like with a relatively high density. Figure 4d and Figure S4a-b (Supporting Information) show the TEM images, which further evidently reveals the peapod-like configuration and where isolated nanoparticles are uniformly distributed in the graphitized carbon fibers. These encapsulated nanoparticles have an average diameter of 30-50 nm. The HRTEM image of the single Ni_2P nanoparticle encapsulated in carbon fibers in Figure 4e and Figure S4c (Supporting Information) show that the marked lattice fringe spacing of 0.221 correspond to the (111) plane of Ni_2P crystal. In addition, from Figure S3b (Supporting Information), well graphitized carbon layers can be feathered with a thickness of 2–4 nm. More importantly, aiming at determining the graphitization in the heat-treated samples, Raman spectroscopy (RS) is also applied (Figure S5, Supporting Information).Compared with the intensities of the D (amorphous carbons) and G (graphitized carbons) bands, it can be confirmed that there presents perfect graphitization in the final samples. Moreover, according to our previous result,[23] a simple method to analyze the carbon content in the peapoded composites material is applied. Results show that the carbon content in the peapods composite is about 11.5 wt%. The X-ray diffraction (XRD) analysis confirms the formation of highly pure Ni_2P crystals with a hexagonal phase (JCPDS No. 74-1385) after annealing (Figure 4f). The crystallographic phase of the inter-connected Ni_2P peapods array growing on Ti foil is also determined by XRD as shown in Figure S2d (Supporting Information). All the diffraction peaks in the XRD patterns can unambiguously be assigned to Ni_2P crystals and Ti foil (JCPDS card no. 44-1294). Furthermore, energy-dispersive X-ray spectrum (EDS) is applied to determine the co-existence of phosphorus and nickel (Figure 4c). Meanwhile, Nitrogen absorption/desorption analysis is applied to investigate the Bruna-uer–Emmett–Teller (BET) surface area of the samples (Figure S6, Supporting Information). The specific surface area for the peapod-like samples could reach 103.8m^2/g and the centered pore size distribution is narrowed at 2.9 nm (Figure S6, inset).

As anode for LIBs, the unique 1D peapods array growing on Ti conductive substrate suggests many potential properties, including large surface-to-volume ratio, easy diffusion of electrolyte into the inner region of the electrode matrix, rapid charge transfer pathway and good mechanical accommodation of strain. Motivated by these interesting structural features, we investigated their electrochemical performance in electrochemical energy storage. The final products on the Ti substrate are scissored into appropriate pieces and directly applied as anode candidate

in LIBs. No other ancillary materials such as carbon black or polymer binder are needed. Figure 5a shows the cyclic voltammograms (CV) of Ni_2P peapods arrays for the first three consecutive cycles at a scan rate of 0.5 mV s^{-1} in the voltage window of 3.0–0.01 V. The CV behavior is generally consistent with those of Ni_2P materials reported in the literature.[25-26] Especially, both of the reduction and oxidation curves almost tend to be stable from the second cycle, indicating that the reversible Li storage occurs in the electrochemical system. Galvanostatic measurements of charge-discharge cyclings are further carried out in the Ni_2P peapods array based on the half-cell configuration at a current density of 200mA g^{-1}, where several representative cycles, including the 1st, 2nd, 50th, and 300th, are displayed (Figure 5b). The initial discharge and charge capacities of the Ni_2P peapods array are about 960 and 637 mAh g^{-1}, respectively, which correspond to a Coulombic efficiency of around 66.3 %.These initial capacities exceed the theoretical value of Ni_2P (542 mAh g^{-1}), which could be ascribed to the decomposition of electrolyte with the formation of a solid-electrolyte-interface (SEI) layer on the electrode surface and extra lithium storage via interfacial charging at metallic interfaces.[26] Such a behavior, i.e. the initial specific capacities exceeding the theoretical values of the active materials, is interesting and has often been reported for other transition metal compound electrodes.[10-12,27-28]

The discharge capacity became much more stable from the second cycle with the Coulombic efficiency of over 95%. After 300 cycles, the discharge capacity is retained as high as 618 mAh g^{-1}, corresponding to ~ 97% of that of the second cycle. It is evident that the 1D Ni_2P@graphitized carbon fiber array shows good cycling performance, which is probably associated with its special peapod-like morphology. This excellent result is comparable to or better than the best reversible capacity previously reported for Ni_2P-based LIB anodes.[25-26] Based on the charge/discharge cycling results shown in Figure 5c, the sample demonstrates extraordinary cyclability, delivering a discharge capacity of ~ 620 mA h g^{-1} during the 300th cycle at a current density of 200 mA g^{-1} with a Coulombic efficiency of ~ 98 %. The superior cycling performance of the nanopeapods array is attributed to its unique structure. Firstly, the thin graphitized carbon fiber layer surrounding the Ni_2P nanoparticles can effectively prevent the adjacent nanoparticles from contacting each other and minimize the aggregation of the particles in the charge/discharge processes. In addition, the carbon layer also constructs an elastic active matrix that can buffer the massive volume expansion and contraction during the repeated electrochemical reactions. Moreover, the active material directly growing on the conductive substrate (Ti foil) can avoid “dead” volume caused by the tedious process of mixing active materials with binders.[29]

The rate capability of Ni_2P peapods array is also explored, as shown in Figure 5d. The assembled cell using peapods array as active materials is first tested at the same charge and discharge current densities of 200 mA g^{-1}, and then at increasing current densities from 600 mA g^{-1} to 10A g^{-1}. We note that the peapods array displays an excellent rate performance. Even at super high rate of 10A g^{-1}, a discharge capacity of 420 mAh g^{-1} can still be achieved, which is the best retention so far for Ni_2P-based anode materials.[22, 25-26]After high-rate testing at 10A g^{-1} for 20 cycles, the current density is reduced to 200 mA g^{-1} and the capacity keeps ascending during the subsequent cycling, almost approaching its initial capacity. To examine the structural stability of the peapods structure, we characterized the morphology of the Ni_2P nanoparticles after charging/discharging at various rates using TEM (Figure S7a, Supporting Information). It is noteworthy that the morphologies and structures of the Ni_2P samples can be generally retained. Meanwhile, there is no obvious breakage, even though the diameters of the nanoparticles increase to about 50-80 nm. In addition, the XRD data (Figure S7b, Supporting Information) certifies that the Ni_2P@graphitized carbon fiber composite still exhibits a crystalline state after charging/discharging at various rates, which is in good agreement with the result of the TEM image. This observation indicates that hierarchical peapods array structure is beneficial to relax the volume expansion and alleviate the active materials agglomeration and pulverization during cycling. Furthermore, the temperature-dependent Li storage performance has been investigated (Figure S8, Supporting Information). As expected, the delivered capacity after 300 cycles at 200mAg^{-1}

gradually increased with the testing temperature varying from 0, to 25 and 50 ^{o}C. As for the novel and unique peapods array, its structural stability during cycling may be responsible for the super rate performance, implying it as a promising anode for high-energy-density LIBs.

One-dimensional (1D) nanostructure on metallic conductive substrate has obtained particularly interest owing to their large specific active surfaces, vectorial charge transport property and strong electronic connection between the active material and current collectors. As shown in Figure 6a, the 1D Ni_2P@graphitized carbon fiber composite peapods array grown directly on Ti substrate affords a hollow channel to facilitate the electrolyte diffusion and abundance of exposed catalytic sites from the dispersive peapods array, which plays an important role in enhancing the electrocatalytic performance in a wide range of electrochemical applications. Motivated by these features, the electrocatalytic activity of as-prepared Ni_2P peapods array (Ni_2P-1) for the hydrogen evolution reaction (HER) is also evaluated in 0.5 M H_2SO_4 electrolyte. For comparison, the Pt/C and random peapod-like Ni_2P/C nanocomposites (Ni_2P-2) are also measured by depositing onto a glassy carbon (GCE, 0.07 mg cm^{-2}) as the working electrode, respectively. In our experiment, the random peapod-like Ni_2P/C nanocomposite (Ni_2P-2) is prepared following the method reported previously.[23] From the polarization curves and Tafel plots (Figure 6a-b), the as-prepared Ni_2P-1 exhibits certain superiority to Ni_2P-2 in both onset potential (~45 *vs.* ~60 mV, *vs.* RHE) and Tafel slope (46 *vs.* 58 mV dec^{-1}), benefiting from the special array structure. The linear regions of the Tafel plots (Figure 6b) fit very well with the Tafel equation $\eta = b \log(j) + a$, where j is the current density and b is the Tafel slope.[13-15,30] Especially, the overpotentials required for the Ni_2P-1catalyst to drive cathodic current densities of 10, 20, and 100 mAcm^{-2} are 54, 85, and 135 mV, respectively, which indicates that the 1D Ni_2P peapods array grown on conductive substrate is an excellent active catalyst for HER.[13-15] Moreover, the temperature-dependent catalytic performance has been tested as well, where the electrocatalytic activity is gradually increased with the temperature varying from 0 to 25 and 50 ^{o}C (Figure S9, Supporting Information). Stability is another important criterion for a good catalyst. To probe the durability of the catalyst in acidic environment, potential sweeps are conducted from -0.5 to 0 V for 5000 cycles. From Figure 6d, it can be seen that the degradation of current density is almost negligible after 1000, 2000 and 5000 cycles. Furthermore, chronoamperometric electrolysis provides evidence of the excellent stability of the as-prepared Ni_2P array. As shown in Figure S10 (Supporting Information), at a low overpotential of 118 mV, the catalyst current density remains stable at~ 40 mA cm^{-2} in electrolysis for 72 h only with a slight loss. This exceptional durability shows a promise for practical applications of the catalysts for the long-term run.

Conclusion

In summary, we have successfully fabricated a novel one-dimensional peapods array of Ni_2P@graphitized carbon fiber composites on Ti foil substrate via a hydrothermal growth and polymerization, followed by annealing in H_2 atmosphere. As a result, the composite electrode displays good cycling stability with 97% capacity retention at 200mA g^{-1} for more than 300 cycles and excellent rate capability with a relatively high capacity of 420 mA h g^{-1} at a high current rate of 10 A g^{-1}, making it a very promising anode candidate for the next-generation advanced LIBs. Additionally, the 1D Ni_2P peapods array grown on Ti foil can be directly used to drive the HER with efficiencies better than many other non-noble-metal catalysts, and simultaneously with wonderful stability under acidic conditions. The superior electrochemical performances of the composite electrodes can be ascribed to several advantages. For instance, the novel 1D peapods array provides effective electrolyte-accessible channels for electrolyte diffusion, and shortens the distance for ionic exchange. Especially, the outer layer of graphitized carbon fiber can not only increase the contact surface area between the electrode and the electrolyte, but also protect the encapsulated nanoparticles from agglomeration. In addition, the direct contact between carbon fibers array and the conductive substrate is favorable for the charge rapid transfer, resulting in an enhanced electrochemical kinetics. Meanwhile, the incorporation of Ti conductive substrate offers the peapods array a good mechanical contact with

the current collectors and is useful to maintain the structural stability in applications. More importantly, this synthesis approach is facile and universal, and can be extended to other systems, thus to open up substantial opportunities for many promising applications, such as energy storage and conversion, sensors, catalysis, and microelectronics.

Experiment Section

Materials: All chemicals or materials were used directly without any further purification before use. Ethylene Glycol (Fisher Chemical, 99.99%), Ammonia Hydroxide (NH_3H_2O, 28–30 wt%, J. T. Baker), Nickel Nitrate ($Ni(NO_3)_2$, 99.9%,Aldrich), Sodium dihydrogen phosphate (NaH_2PO_4, 99.9%), Sodium Carbonate (Na_2CO_3, 99.9%, Aldrich), D(+)-Glucose (Cica-Reagent, Kanto Chemical), sulfuric acid （99.999%）, metallic Li foil (99.9 %, Aldrich) and Ti foil (0.127 mm (0.005 inch) thick, annealed, 99%, Alfa Aesar) , were used as received .

Synthesis of $NH_4NiPO_4H_2O$ nanobelt array on Ti foil.

Prior to the synthesis, a Ti foil with size of 1×3 cm was rinsed with D.I. water and pure ethanol subsequently or sonically cleaned by a mixture of D.I. water, ethanol and acetone with volume ratio of 1:1:1 for 10 min. Afterwards, the Ti foil was tilted against the wall of the autoclave at a certain angle, with the interested surface facing down. A little modified solution composed of ethylene glycol (10 mL), concentrated NH_3H_2O (10 mL, 28–30 wt %), an aqueous solution of $Ni(NO_3)_2$ (5 mL, 1 M), an aqueous solution of NaH_2PO_4 (7.5 mL, 1 M), and an aqueous solution of Na_2CO_3 (5 mL,1 M), was slowly poured into the autoclave. The autoclave was then tightly sealed and left in an oven at 170 ℃ for 24 hrs for reaction. Once the reaction was over, the Ti foil was taken out and dried in a vacuum oven at 40 ℃for at least 3 hrs.

Preparation of Ni_2P peapods array on Ti foil.

Ti foil with $NH_4NiPO_4H_2O$ nanobelts array covered was tightly tilted against the inner wall of a clean 45 ml Teflon liner. Then glucose aqueous solution (3 ml, 1 M) was mixed with additional D.I. water (27 ml) to form a homogeneous solution after 5 min ultrasonication. The above solution was introduced into the above-mentioned 45 ml Teflon-lined autoclave and sealed tightly. Then the liner was heated in an electric oven at 180℃ for 4 hrs. After that, we washed the Ti foil using D. I. water and ethanol, and dried the foil in air at 60℃ overnight to remove the residue water and ethanol. Afterwards, the dried samples were loaded into the tube furnace and calcined in H_2 atmosphere at 700~750℃ for 200 min with a ramp of 1℃/min.

Characterization

Measurements using scanning electron microscopy (SEM) were conducted with a JEOL JSM-7800F. Transmission electron microscopy (TEM) and high-resolution TEM (HRTEM) observations were carried out (Philips, Tecnai, F30) at 300 kV. These observations were coupled with energy-dispersive X-ray spectrometry (EDX). The X-ray diffraction (XRD) patterns were recorded with a Rigaku Rotalflex RU-200B diffractometer using a Co−K_α (λ = 1.5418 Å) source with a Ni filter at 40 kV, 40 mA, and a scan rate of 0.02° s^{-1}.

Electrochemical measurements

Lithium-ion batteries: The Ni_2P peapods arrays on the Ti substrates were directly employed as a working electrode without addition of any conductive agents or cohesive binders. The mass of the as-prepared Ni_2P arrays was measured using a microbalance (Sartorius, BT 125D) by weighing the sample before and after the synthesis process. Prior to the battery cycling tests, the electrode was dried in a vacuum oven overnight at 120 °C. The electrolyte consisted of 1 M $LiPF_6$ in a 1:1 v/v mixture of ethylene carbonate and diethyl carbonate (Cheil Industries). Pure lithium foil was used as a counter electrode, and Cellgard 2400 was used as a separator film. The cell was assembled in an argon-filled glovebox where moisture and oxygen concentrations were strictly limited to below 0.1ppm. Galvanostatic charge–discharge tests were conducted on LAND battery program-control test system (CT-2001A, Jinnuo electronic Co.). Cyclic voltammogram (CV) tests were performed on a CHI660D electrochemistry workstation (Chenhua Instrument Co.) at a scan rate of 0.1 mV/s between 0.01 and 3.0 V vs. Li/Li^+.

Hydrogen evolution reaction: Electrochemical measurements are performed with a CHI660D electrochemical workstation (CH Instruments, Inc., Shanghai). A three-electrode cell is used, including an active material as the

working electrode, a saturated calomel electrode (SCE) as the reference electrode, and a platinum wire as the counter electrode. Ni_2P peapods array grown on Ti foil is directly applied as a working electrode, with only a defined area (0.07 cm^2) of the front surface of the sample exposed to solution during measurements. The Pt/C catalyst or peapod-like Ni_2P/C nanocomposites and Nafion solution (5 wt %, 80 μ L) were dispersed in 1 mL of water/ethanol (3:1, v/v) by ultrasonication to form a homogeneous ink. Then 5 μL of catalyst ink was loaded onto a glassy carbon electrode (~loading: ~0.36 mg cm^2).Linear sweep voltammetry (LSV) was performed in solution of 0.5 M H_2SO_4 with a scan rate of 5 mV s^{-1} in a range from -0.2 V to -0.5 V. Durability test was then carried out by cyclic voltammetry (CV) scanning from -0.5 to 0 vs. SCE for 5000 at a scan rate of 50 mV s^{-1}. In all measurements, (SCE) was used as the reference, and all the potentials reported in our work were vs. the reversible hydrogen electrode (RHE). In 0.5 M H_2SO_4, E (RHE) = E (SCE) + 0.281 V.[31]

Acknowledgements

This work was financially supported by the Thousand Young Talents Program of the Chinese Central Government (Grant No.0220002102003), National Natural Science Foundation of China (NSFC, Grant No. 21373280，21403019), Beijing National Laboratory for Molecular Sciences (BNLMS) and Hundred Talents Program at Chongqing University (Grant No. 0903005203205).

Supporting Information Available: Details of experiments and additional supplementary figures about this paper.

References and Notes:

1. S. Carenco, D. Portehault, C. Boissiere, N. Mezailles and C. Sanchez, *Chem Rev*, 2013, **113**, 7981-8065.
2. Y. Nakagawa, H. Kageyama, Y. Oaki and H. Imai, *J. Am. Chem. Soc.*, 2014, **136**, 3716-3719.
3. V. Chabot, D. Higgins, A. P. Yu, X. C. Xiao, Z. W. Chen and J. J. Zhang, *Energ Environ. Sci*, 2014, **7**, 1564-1596.
4. M. S. Faber, R. Dziedzic, M. A. Lukowski, N. S. Kaiser, Q. Ding and S. Jin, *J. Am. Chem. Soc.*, 2014, **136**, 10053-10061.
5. Y. Wang, Y. J. Bai, X. Li, Y. Y. Feng and H. J. Zhang, *Chem. Eur. J.*, 2013, **19**, 3340-3347.
6. B. You, J. H. Jiang and S. J. Fan, *ACS Appl. Mater. Interfaces.*, 2014, **6**, 15302-15308.
7. R. Liu, F. L. Qu, Y. L. Guo, N. Yao and R. D. Priestley, *Chem. Commun.*, 2014, **50**, 478-480.
8. H. J. Zhang, Y. Y. Feng, Y. Zhang, L. Fang, W. X. Li, Q. Liu, K. Wu and Y. Wang, *Chemsuschem.*, 2014, **7**, 2000-2006.
9. M. M. Ye, S. Zorba, L. He, Y. X. Hu, R. T. Maxwell, C. Farah, Q. Zhang and Y. D. Yin, *J. Mater. Chem.*, 2010, **20**, 7965-7969.
10. H. J. Zhang, Y. J. Bai, Y. Zhang, X. Li, Y. Y. Feng, Q. Liu, K. Wu and Y. Wang, *Sci. Rep.*, 2013, **3**: 2717.
11. S. Saadat, J. X. Zhu, D. H. Sim, H. H. Hng, R. Yazami and Q. Y. Yan, *J. Mater. Chem. A.*, 2013, **1**, 8672-8678.
12. X. Y. Xue, S. A. Yuan, L. L. Xing, Z. H. Chen, B. He and Y. J. Chen, *Chem. Commun.*, 2011, **47**, 4718-4720.
13. Z. B. Chen, D. Cummins, B. N. Reinecke, E. Clark, M. K. Sunkara and T. F. Jaramillo, *Nano Lett*, 2011, **11**, 4168-4175.
14. J. Q. Tian, Q. Liu, N. Y. Cheng, A. M. Asiri and X. P. Sun, *Angew. Chem. Int. Ed.*, 2014, **53**, 9577-9581.
15. Z. P. Huang, Z. B. Chen, Z. Z. Chen, C. C. Lv, H. Meng and C. Zhang, *Acs Nano.*, 2014, **8**, 8121-8129.
16. R. H. Lin and Y. J. Ding, *Materials.*, 2013, **6**, 217-243.
17. Z. H. Pu, Q. Liu, P. Jiang, A. M. Asiri, A. Y. Obaid and X. P. Sun, *Chem. Mater.*, 2014, **26**, 4326-4329.
18. K. L. Li, R. J. Wang and J. X. Chen, *Energy Fuels.*, 2011, **25**, 854-863.
19. G. H. L. Savithra, E. Muthuswamy, R. H. Bowker, B. A. Carrillo, M. E. Bussell and S. L. Brock, *Chem Mater*, 2013, **25**, 825-833.
20. X. Li, M. H. Lu, A. J. Wang, C. S. Song and Y. K. Hu, *J. Phys. Chem. C.*, 2008, **112**, 16584-16592.
21. E. J. Popczun, J. R. McKone, C. G. Read, A. J. Biacchi, A. M. Wiltrout, N. S. Lewis and R. E. Schaak, *J. Am. Chem. Soc.*, 2013, **135**, 9267-9270.
22. a) Y. Lu, C. D. Gu, X. Ge, H. Zhang, S. Huang, X. Y. Zhao, X. L. Wang, J. P. Tu and S. X. Mao, *Electrochim. Acta*, 2013, **112**, 212-220; b) Y. Lu, J. P. Tu, Q. Q. Xiong, Y. Q. Qiao, X. L. Wang, C. D. Gu, S. X. Mao, *RSC Adv.*, 2012, **2**, 3430-3436; c) Y. Lu, J. P. Tu, C. D. Gu, X. L. Wang, S. X. Mao, *J. Mater. Chem.*, 2011, **21**, 17988- 17997.
23. Y. J. Bai, H. J. Zhang, X. Li, L. Liu, H. T. Xu, H. J. Qiu, Y. Wang., *Nanoscale*,. 2014, 7, 1446 - 1453.
24. H. S. Lee, T. Hur, S. Kim, J. H. Kim and H. I. Lee, *Catal Today.*, 2003, **84**, 173-180.
25. H. Zhang, Y. Lu, C. D. Gu, X. L. Wang and J. P. Tu, *CrystEngComm.*, 2012, **14**, 7942-7950.
26. Y. Lu, J. P. Tu, Q. Q. Xiong, Y. Q. Qiao, J. Zhang, C. D. Gu, X. L. Wang and S. X. Mao, *Chem. Eur. J.*, 2012, **18**, 6031-6038.
27. J. Liu, H. Xia, D. F. Xue and L. Lu, *J. Am. Chem. Soc.*, 2009, **131**, 12086-12087.
28. S. M. Xu, C. M. Hessel, H. Ren, R. B. Yu, Q. Jin, M. Yang, H. J. Zhao and D. Wang, *Energ Environ. Sci.*, 2014, **7**, 632-637.
29. Y. G. Li, B. Tan and Y. Y. Wu, *Nano Lett*, 2008, **8**, 265-270.

30. P. Xiao, M. A. Sk, L. Thia, X. M. Ge, R. J. Lim, J. Y. Wang, K. H. Lim and X. Wang, *Energ Environ. Sci.*, 2014, **7**, 2624-2629.

31. W. Cui, N. Y. Cheng, Q. Liu, C. J. Ge, A. M. Asiri and X. P. Sun, *ACS Catal.*, 2014, **4**, 2658-2661.

Figures and Captions

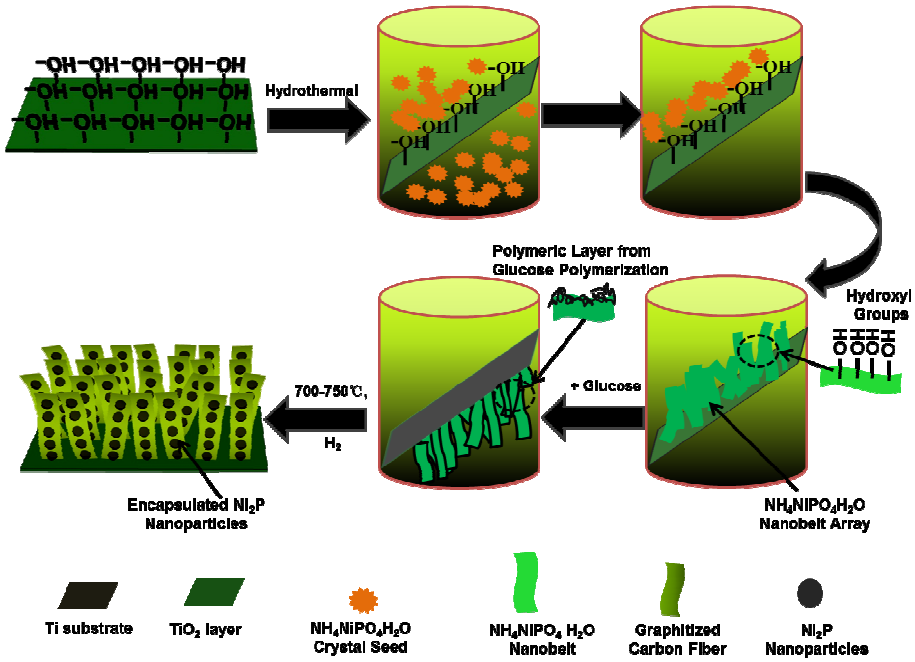

Figure 1. Schematic illustration of the preparation process of 1D Ni_2P@graphitized carbon fiber peapods array.

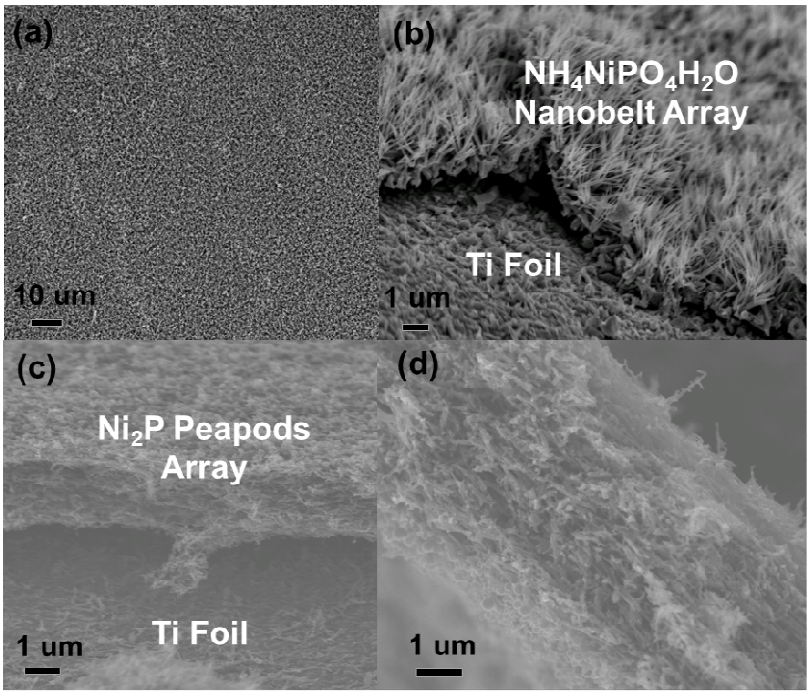

Figure 2. a) Top-view and b) cross –section SEM images of $NH_4NiPO_4H_2O$ nanobelts on Ti foil，which suggests the formation of uniform nanobelt arrays on a large area. c – d) Cross – section SEM images of Ni_2P peapods array on Ti foil substrate.

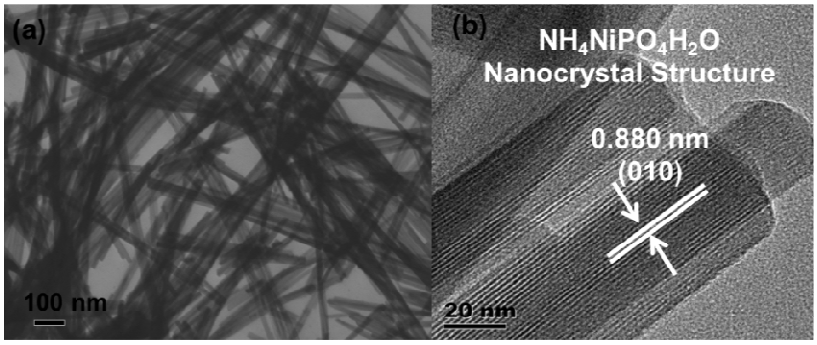

Figure 3. Representive SEM and TEM images of the $NH_4NiPO_4H_2O$ nanobelts scraped down from Ti foil by the powerful ultrasound technology: a) SEM image of the product; b) HRTEM image of the well-crystallized nanobelts.

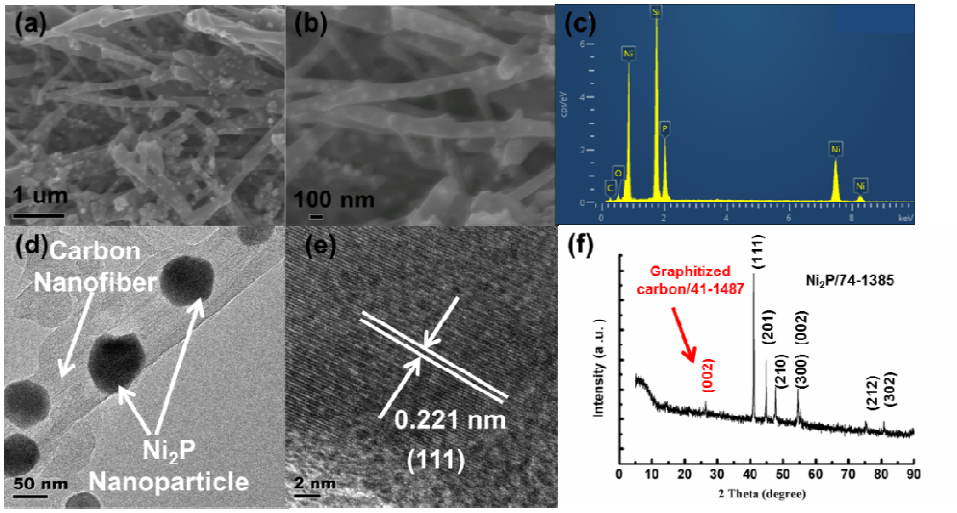

Figure 4. a, b) SEM images of Ni_2P peapods obtained after calcination at 700℃ under H_2 atmosphere. c, d, e and f) EDS, TEM, HRTEM and XRD images of the Ni_2P peapods scraped down from Ti foil by the powerful ultrasound technology, respectively.

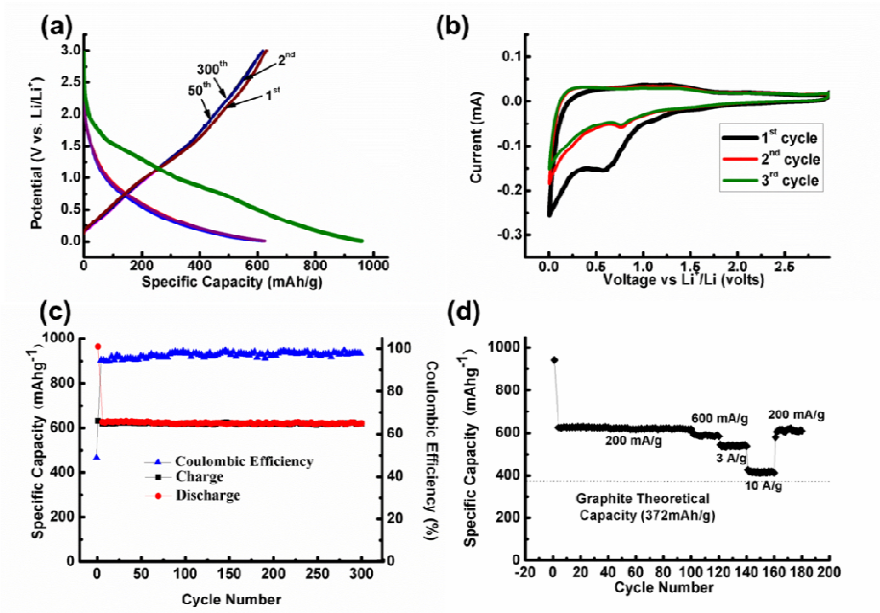

Figure 5. Lithium ion battery performances of the Ni_2P peapods array electrodes. a) Cyclic voltammograms and b) the cycle galvanostatic charge and discharge voltage profiles cycled between 3 and 0.01 V at a current density of 0.2 A g^{-1}; c) the cycling performance and Coulombic efficiency cycled at a current density of 0.2 A g^{-1}; d) rate capabilities of the samples at various rates.

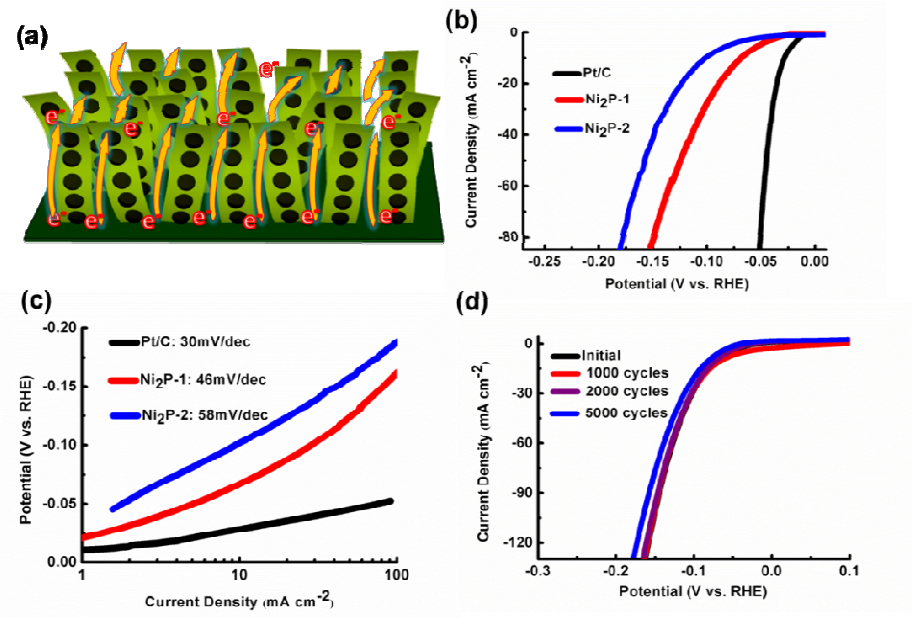

Figure 6. a) The schematic illustrations of the Ni_2P@graphitized carbon fiber composite peapods array (Ni_2P-1) with possible electrolyte flow path, which shows that the space between the peapod arrays serves as a mass flow channel for the electrolyte diffusion. b, c)Polarization data and Tafel plots for Ni_2P-1, peapod-like Ni_2P nanocomposites (Ni_2P-2) and Pt in 0.5 M H_2SO_4, respectively. d) Polarization curves for Ni_2P-1 electrode (0.38 mg cm^{-2} mass loading) in 0.5 M H_2SO_4 with a scan rate of 50 mV/s initially and after 5000 cycles between 0 and -0.5 V vs. RHE.